Formisano & Lombardi, *Cogent Engineering* (2016), 3: 1156279
http://dx.doi.org/10.1080/23311916.2016.1156279

cogent engineering

CIVIL & ENVIRONMENTAL ENGINEERING | RESEARCH ARTICLE

Numerical prediction of the non-linear behaviour of perforated metal shear panels

A. Formisano[1*] and L. Lombardi[1]

Received: 25 October 2015
Accepted: 09 February 2016
First Published: 15 March 2016

*Corresponding author: A. Formisano, Department of Structures for Engineering and Architecture, University of Naples "Federico II", P.le Tecchio 80, 80125 Naples, Italy
E-mail: antoform@unina.it

Reviewing editor:
Amir H. Alavi, Michigan State University, USA

Additional information is available at the end of the article

Abstract: Steel plate shear walls (SPSWs) are innovative systems able to confer to either new or existing structures a significant capacity to resist earthquake and wind loads. Many tests have shown that these devices may exhibit high strength, initial stiffness and ductility, as well as an excellent ability to dissipate energy. When full SPSWs are used as bracing devices of buildings, they may induce excessive stresses in the surrounding main structure where they are inserted, so to require the adoption of large cross section profiles. For this reason, perforated steel panels, which are weakened by holes aiming at limiting the actions transmitted to the surrounding frame members, represent a valid alternative to full panels. In this work, aiming at showing the advantages of such devices, a FEM model of perforated panels has been calibrated on the basis of recent experimental tests. Subsequently, a parametric FEM analysis on different series of perforated panels, by changing the number and diameter of the holes, the plate thickness and the metal material, has been carried out. Finally, the achieved numerical results have been used to set up design charts to correctly estimate the strength and stiffness of perforated metal shear panels.

Subjects: Iron; Steel & Metals Industries; Software Engineering & Systems Development; Structural Engineering

Keywords: steel plate shear walls; perforated panels; circular holes; FEM analysis; parametric analysis; design charts

ABOUT THE AUTHORS

A. Formisano is assistant professor of Structural Engineering from 2007 and Aggregate Professor of Structural Design from 2014 at the same faculty. He is involved in numerous research projects and he is author of more than 180 papers mainly published in conference proceedings and journals dealing with steel and aluminium structures, seismic and volcanic vulnerability, retrofitting, robustness, sustainability and fire resistance. He is an editorial board member and reviewer of numerous international conferences and scientific journals. He was reviewer of the design standards on steel structures and actually he is a project team member of the SC9.T2 task "New types of connections" of the EN 1999-1-1 code.

L. Lombardi is graduated from University of Naples "Federico II" in Structural and Geotechnical Engineering. His research areas of interest include Seismic Design and Seismic Retrofitting of RC and steel building structures. Currently, he is PhD student in Civil Engineering at the University of Bristol.

PUBLIC INTEREST STATEMENT

This study aims to examine a new passive control device based on perforated metal shear panels (PMSPs). Such a technique is particularly advantageous for seismic retrofitting of rc and steel buildings, designed according to obsolete design codes, which are particularly vulnerable to earthquakes. In this framework, PMSPs are highly competitive with the common intervention techniques, since they can increase simultaneously the performance of the buildings in terms of lateral strength, initial stiffness, ductility and dissipated energy. A controlled weakening of the plates by means of different drilling configurations allows to reduce the internal forces in the existing structures and, as a consequence, the additional reinforcement of their members. In this paper, a FEM model based on literature experimental tests is set up for the analysis of such devices. Design charts for the estimation of shear strength and initial stiffness of PMSPs are proposed in order to encourage practitioners to use them.

1. Introduction

The seismic protection systems based on the use of steel plate shear walls (SPSWs) consist of stiff horizontal and vertical boundary frame elements and infill plates. SPSWs possess good ductility and high energy dissipation capability under cyclic loading and have high initial stiffness, so resulting very effective in limiting the inter-storey drift of framed buildings. In addition, by using shop-welded or bolted connection type, the erection process can be ease, allowing a considerable reduction in constructional costs.

There are two types of SPSWs, namely the "standard system" and the "dual system" (Astaneh-Asl, 2000). In the "standard system", SPSWs are used as the lateral load-resisting system only, so that beams and columns are unique components designed to transfer vertical loads. In the "dual system", also the boundary members, generating a moment resisting frame, contribute to resist horizontal loads. Generally, these systems are located in perimeter frames of the main structure or around staircases, they occupying an entire span or a part thereof. Moreover, they can be stiffened or unstiffened, depending on the design philosophy. In the first case, SPSW may be provided with bending stiffeners, which improve the structure dissipative behaviour. Alternatively, the same behaviour can be attained using low yield strength metals, namely low yield steel (De Matteis, Formisano, Mazzolani, & Panico, 2005) or aluminium (Formisano, Mazzolani, Brando, & De Matteis, 2006), as base materials for plates. Contrary, when unstiffened thin panels are used, they immediately buckle under in-plane loads, but additional loads can be carried due to the tension field mechanism, which develops under form of tensile strips in the plate diagonal main directions (Basler, 1961). As a consequence, the boundary frame members have to be designed to support this mechanism developed by the plate. From recent researches, it was found that the panel ideal behaviour is obtained for width/height ratios between 0.8 and 2.5 (Formisano, Mazzolani, & De Matteis, 2007). The tension field action may induce in the frame members large forces demands, which give rise to the adoption of high-depth profiles. A number of solutions have been proposed to provide an answer to this problem, based on either connection of the infill plate to the beams only (Xue & Lu, 1994), or plates with vertical slits (Hitaka & Matsui, 2003), or thin light-gauge cold-rolled steel panels (Berman & Bruneau, 2005; Formisano, De Matteis, Panico, Calderoni, & Mazzolani, 2006; Formisano, De Matteis, Panico, & Mazzolani, 2008; Formisano & Sahoo, 2015), or low-yield strength steel panels (Mistakidis, De Matteis, & Formisano, 2007), or perforated plates (Purba & Bruneau, 2007), or aluminium plates (Brando & De Matteis, 2014; De Matteis, Formisano, & Mazzolani, 2009; Formisano, De Matteis, & Mazzolani, 2010).

In this paper, the attention is focused on the use of perforated SPSWs, in order to limit the construction cost deriving from the installation of such devices into the structure. Therefore, a FEM model, implemented with ABAQUS (Dassault Systèmes, 2010) and calibrated on the basis of the previous literature experimental tests on panels with a central hole (Valizadeh, Sheidaii, & Showkati, 2012), has been developed in order to set up a parametric analysis on devices having different configurations of holes.

In conclusion, the achieved numerical results have been used to propose analytical tools, under form of design charts, for evaluating both the shear capacity and the initial stiffness of perforated metal shear panels.

2. State-of-the-art on unstiffened perforated panels

The first studies aimed at evaluating the behaviour of unstiffened full SPSWs were presented by Thorburn, Kulak, and Montgomery (1983), who proposed two numerical methods called the "Equivalent Truss Model" and the "Strip Model" for analysis of these multi-storey systems.

On the basis of experimental diagonal tests performed on SPSWs within a pinned joint frame, Roberts and Sabouri-Ghomi (1991) proposed a theoretical method, namely the Plate-Frame Interaction method, for calculating the shear capacity F_{wu} and the stiffness K_w of the steel plate device. The contribution of the plates only can be obtained through the following equations:

$$F_{wu} = bt\left(\tau_{cr} + \frac{1}{2}\sigma_{ty}\sin 2\vartheta\right) \tag{1}$$

$$K_w = \frac{\left(\tau_{cr} + \frac{1}{2}\sigma_{ty}\sin 2\vartheta\right)}{\left(\frac{\tau_{cr}}{G} + \frac{2\sigma_{ty}}{E\sin 2\vartheta}\right)}\frac{bt}{d} \tag{2}$$

where t, b and d are the thickness, width and height of the steel plate, respectively, E and G are the Young and Shear elasticity moduli of the steel plate materials, σ_{ty} is the tension field stress in the plate yielding condition, ϑ is the diagonal tension field angle, measured from the horizontal direction and τ_{cr} is the critical buckling shear stress, evaluated according to the Timoshenko and Gere's theory (1961).

Performing experimental tests on panels with a central opening, Roberts and Sabouri-Ghomi (1992) proposed an empirical reduction factor $\left(1-\frac{D}{d}\right)$, where D is the opening diameter and d is the panel depth, to reduce the SPSW strength and stiffness given in Equations 1 and 2 due to the hole presence. The authors also proposed to use a new reduction coefficient $\left(1-\frac{A}{A_0}\right)$, where A is the opening area and A_0 is the plate area, instead of the above one.

Sabouri-Ghomi, Ventura, and Kharrazi (2005) modified Equations 1 and 2 by introducing two modification factors, namely C_{m1} and C_{m2}, accounting for beam-to-column connections, plate-to-frame connections and the effect of both flexural behaviour and stiffness of boundary elements. By applying the above modification factors, Equations 1 and 2 become:

$$F^*_{wu} = bt\left(\tau_{cr} + \frac{C_{m1}}{2}\sigma_{ty}\sin 2\vartheta\right) \tag{3}$$

$$K^*_w = \frac{\left(\tau_{cr} + \frac{C_{m1}}{2}\sigma_{ty}\sin 2\vartheta\right)}{\left(\frac{\tau_{cr}}{G} + \frac{2C_{m2}\sigma_{ty}}{E\sin 2\vartheta}\right)}\frac{bt}{d} \tag{4}$$

where the modification factors were limited as follows: $0.8 < C_{m1} < 1.0$ and $1.0 < C_{m2} < 1.7$. The authors recognized that these values will need further refinement as more test results will become available in the future.

Purba and Bruneau (2007) experimentally tested a 4,000 × 2,000 mm shear panel with a configuration of 20 regularly spaced circular holes. The panel, made of low yield strength steel, had reduced beam sections at the ends. Utilizing a steel thin panel with low-yield strength, the Authors observed that both the device strength was reduced and the energy dissipation was anticipated. It was also found that, for multiple regularly spaced perforations, Equation 1 provided a conservative estimate of the perforated infill plate strength when d is replaced by S_{diag}, that is the diagonal distance between two consecutive perforation lines. So, through a FEM model calibrated on the experimental results, the following modified equation to calculate the shear strength of perforated shear panels with regular perforation patterns was proposed:

$$F_{wu,perf} = F_{wu}\left(1 - 0.7\frac{D}{S_{diag}}\right) \tag{5}$$

Moreover, by studying a plate portion, the researchers observed that analysis results on an individual perforated strip can accurately predict the behaviour of a complete perforated SPSW, provided that the hole diameter is less than 60% of the strip width.

A series of unstiffened SPSWs with different perforation patterns were investigated by Bhowmick, Grondin, and Driver (2014). On the basis of analytical considerations, the Authors showed that the shear strength of an infill plate with circular perforations can be calculated by the following equation:

$$F_{wu,perf} = F_{wu}\left(1 - \beta N_r \frac{D}{L_p \cos\alpha}\right) \quad (6)$$

where α is the tension field angle, D is the circular hole diameter, L_p is the width of perforated infill plate, N_r is the maximum number of diagonal strips and β is a regression constant, obtained from a FEM analysis, to fit the system behaviour. Eight regular perforation patterns and three diameters of the holes were considered. It was shown that a value of 0.7 can be assumed for the constant β, except for plates with a central hole, for which a value of 1.35 should be used. As a result, an excellent agreement between the FEM analysis results and the device shear strength prediction resulted from Equation 6 was observed.

In 2012, eight 1:6 scaled test specimens with a central circular hole, having two plate thicknesses and four D/b ratios (D = hole diameter and b = panel width), were tested under cyclic loading by Valizadeh et al. (2012). The obtained experimental results showed a stable behaviour of the panels for large displacements up to a drift of 6%. It was also observed that, during the loading phase, the stable cyclic behaviour of specimens in the non-linear range mostly caused a dissipation of energy, but the presence of an opening at the panel centre provoked a noticeable decrease in the system energy absorption. During the test program, specimens without opening, due to their higher ultimate strength, showed a bearing failure of the plate-to-connection system near the corner. In perforated specimens with lower plate thickness, plate tearing failure occurred around the opening due to the stress concentration.

3. Numerical studies on unstiffened perforated panels

3.1. The proposed FEM model

The existing experimental studies on perforated SPSWs gave significant contributions to understand the effective behaviour of such systems. However, the relevant geometrical and mechanical parameters of SPSWs investigated in laboratory tests did not allow to cover all possible panel configurations which can be used in practice. For this reason, a FEM model of such devices is herein implemented in ABAQUS (Dassault Systèmes, 2010) for simulating their behaviour under monotonic and cyclic loading. In order to focus attention on the behaviour of the plate only, the proposed FEM model has been set up on panels within pinned joint frames made of UPN120 coupled profiles (see Figure 1), as in the already mentioned experimental test of Valizadeh et al. (2012).

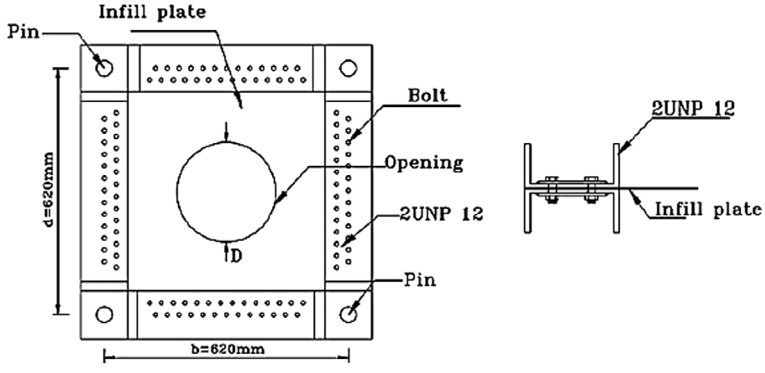

Figure 1. Geometrical representation of the specimens tested by Valizadeh et al. (2012).

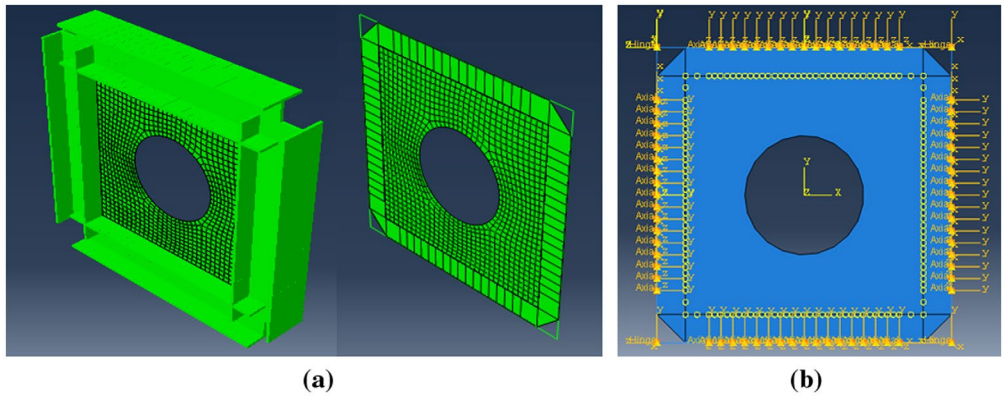

Figure 2. Proposed FEM model in ABAQUS (Dassault Systèmes, 2010): mesh (a) and boundary conditions (b).

Both the plate and the frame are modelled with 3D deformable elements. In particular, plate is modelled by S4R shell elements, while frame members are modelled with B31 beam elements (Figure 2(a)). The beam-to-column frame connections are modelled by HINGE connectors. Through a preliminarily sensitivity analysis, an approximate mesh size of 15 mm is chosen for the plate. Due to the presence of holes, a more dense mesh around them is required in order to both discretize properly the surface and introduce a sufficient number of cells between near holes. About boundary conditions, at the base the frame is restrained with fixed hinges. Instead, the upper beam is constrained towards out-of-plane displacements in order to simulate the presence of lateral supports in that direction. The plate-to-frame connections are modelled by AXIAL connectors. For simplicity, an equivalent centroid row of connectors for each panel side, instead of the double rows used in the experimental test, is adopted (Figure 2(b)). The contact between the two UPN120 profiles and the plate is simulated by restraining the out-of-plane displacement of the plate in an extended area of 60 mm from its edges. The mesh is diversified in this plate area, in comparison to that used for the plate, to reflect the real location of the bolts.

The model takes into account the geometrical and mechanical non-linearities of the system. The plate is modelled by an elastic–plastic-hardening material. In particular, an isotropic hardening is used for the monotonic analysis, while a combined hardening model is used for cyclic analysis. On the other hand, the frame members are modelled by an elastic material, since no yielding is expected for them.

When plates are subjected to in-plane actions, their behaviour is affected by out-of-plane deformations. In fact, perfectly plane plates exhibit high stiffness under in-plane actions but, if affected by even small initial imperfections, they can exhibit substantially lower stiffness. These imperfections may be derived from either manufacture or installation processes. In order to take into account the initial imperfections of the plates, deformed shapes related to the plate instability modes are assigned to the SPSWs. Moreover, some imperfections due to bolted connections localized along the panel perimeter (hole spacing, bolt-hole clearance, tightening pressure) are introduced in the FEM model. It is possible to take into account for these imperfections by means of AXIAL connectors, whose behaviour is opportunely calibrated on the basis of the experimental evidences (Valizadeh et al., 2012).

A sensitivity analysis has shown that, using a perfect plate-to-frame connection with the TIE function of ABAQUS, a stiffness greater than the experimental one is achieved. Contrary, first by properly calibrating the behaviour of the AXIAL connectors and then by assuming an initial imperfection of the plates with a deformed shape related to the first instability mode with amplitude equal to 1 mm, the experimental behaviour of the system is realistically simulated (Figure 3).

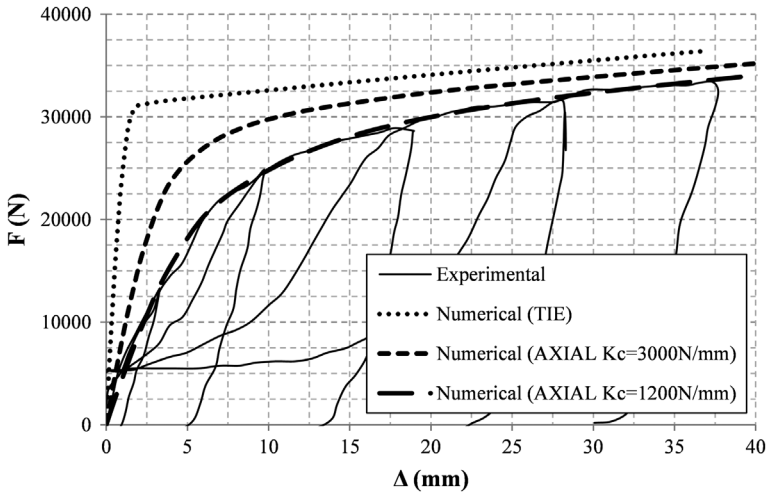

Figure 3. Calibration of the connectors behaviour.

3.2. The FEM model calibration

The FEM model previously described is calibrated by comparing the predictive behaviour to the test results of Valizadeh et al. (2012). This operation is necessary to take into account all imperfections and uncertainties that inevitably afflict the real experiments. In these tests, eight panels filling a hinged joint frame were considered. The centreline-to-centreline spacing between the two coupled UPN120 beams and columns of the frame was set equal to 620 mm (Figure 1). However, the geometrical dimensions of internal plates were assumed equal to 500 × 500 mm, by considering the depth of the applied channel sections of the framing system. The properties of experimental specimens are listed in Table 1. Experimental specimens were tested under a cyclic loading process with five cycles up to a drift of 6%.

For the sake of brevity, just some of the obtained results are reported in the following. An initial out-of-plane imperfection proportional to the first instability mode with amplitude of 1 mm is assigned to all panels, based on a preliminary sensitivity analysis (Formisano & Lombardi, 2015). The panel numerical behaviour has been experimentally calibrated on the basis of the axial stiffness of the connectors. In particular, the SPW3 panel is calibrated by adopting an axial stiffness of the connectors K_c equal to 1,200 N/mm. This panel has shown, both experimentally and numerically, to attain a maximum drift of 6% without failure. The experimental-to-numerical comparison in terms of both hysteretic curves and deformed shape is shown in Figure 4.

The SPW7 specimen, more slender than the SPW3 one, is calibrated by adopting an axial stiffness of the connectors K_c equal to 1,500 N/mm. This panel has shown, both experimentally and

Table 1. Features and failure modes of specimens experimentally tested by Valizadeh et al. (2012)

Specimen	Thickness (mm)	Opening (mm)	f_{ym} (MPa)	f_{um} (MPa)	Failure mode
SPW1	0.70	–	180	300	Plate-frame connection
SPW2	0.70	100	180	300	No failure
SPW3	0.70	175	180	300	No failure
SPW4	0.70	250	180	300	No failure
SPW5	0.37	–	299	375	Plate-frame connection
SPW6	0.37	100	299	375	Fractures around hole
SPW7	0.37	175	299	375	Fractures around hole
SPW8	0.37	250	299	375	No failure

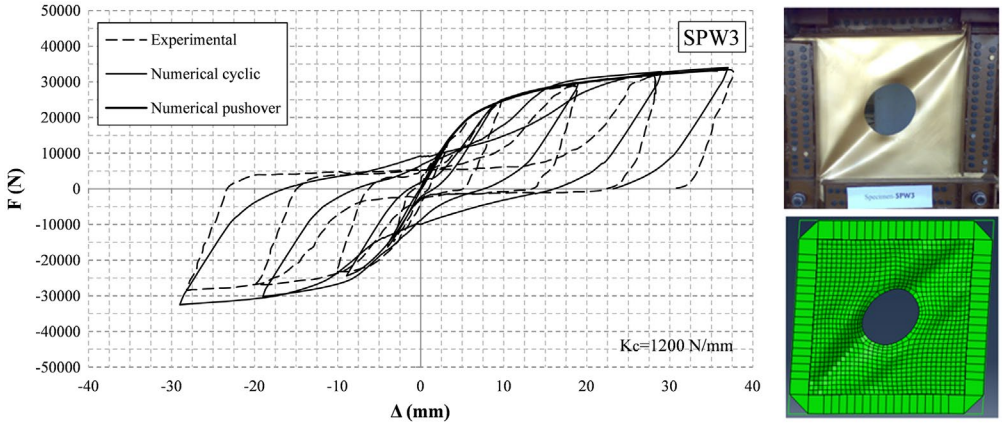

Figure 4. Numerical calibration of experimental results on the SPW3 specimen tested by Valizadeh et al. (2012) and comparison in terms of deformed shape.

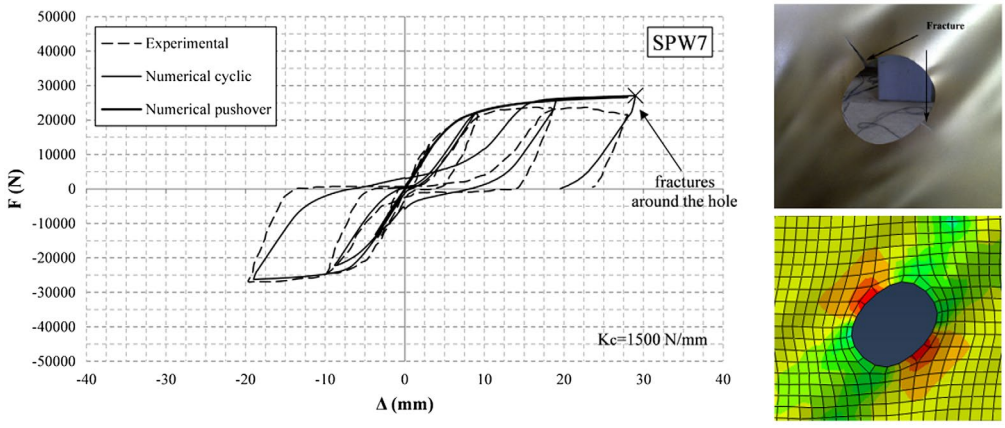

Figure 5. Numerical calibration of experimental results on the SPW7 specimen tested by Valizadeh et al. (2012) and comparison in terms of stress concentration.

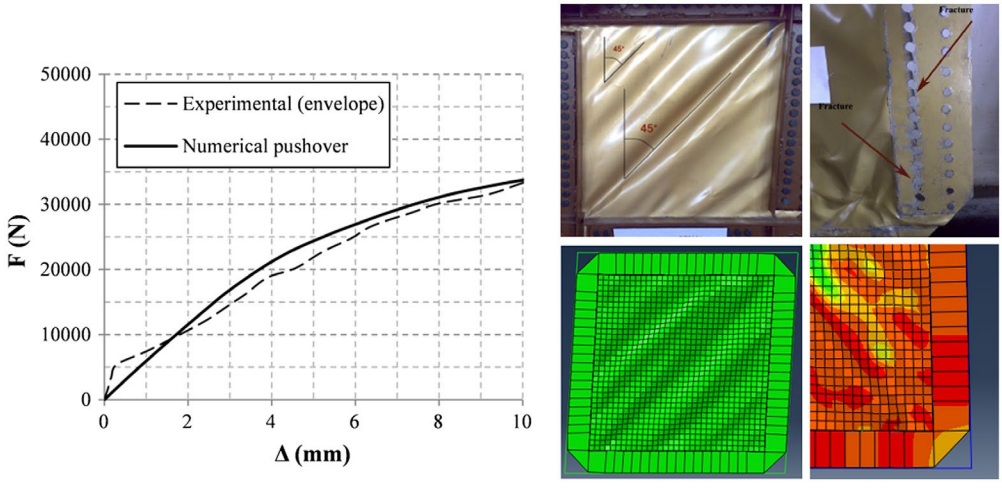

Figure 6. Experimental-numerical comparison of force-displacement curves and numerical calibration in terms of both deformed shape and stress concentration related to the SPW1 specimen tested by Valizadeh et al. (2012).

numerically, to attain a maximum drift of about 4% with fractures around the hole. From the experimental-to-numerical comparison in terms of hysteretic curves (Figure 5), a little discrepancy is noticed in the post-peak strength phase. A better accuracy in the panel resistance prediction would be possible if the opening of fractures is modelled with a more refined theoretical model. However, the model is able to satisfactory simulate the stress concentration around the hole.

Table 2. Summary of the results obtained from the model calibration

Specimen	K_c (KN/m)	$K_{i,exp}$ (KN/m)	$K_{i,num}$ (KN/m)	Var K_i (%)	$F_{max,exp}$ (KN)	$F_{max,num}$ (KN)	Var F_{max} (%)	$E_{d,tot,exp}$ (KN/m)	$E_{d,tot,num}$ (KN/m)	Var $E_{d,tot}$ (%)
SPW1	1,500	4,870	5,260	8	–	–	–	–	–	–
SPW2	1,200	4,400	4,524	3	34.80	36.58	5	1.77	1.59	−11
SPW3	1,200	4,225	4,057	−4	33.10	34.04	3	2.59	2.68	4
SPW4	1,000	3,866	3,535	−9	25.00	25.52	2	1.70	1.54	−10
SPW5	1,500	5,118	4,960	−3	–	–	–	–	–	–
SPW6	1,300	3,900	3,801	−3	25.90	29.25	13	0.90	0.81	−11
SPW7	1,500	4,158	3,765	−10	24.60	27.09	10	1.10	1.09	−1
SPW8	1,500	4,077	3,255	−25	20.10	19.08	−5	1.10	0.83	−32

The SPW1 panel has experimentally shown a failure at the plate-to-frame connections. This failure mode has strongly penalized its behaviour during the test. However, the initial behaviour of the panel before the failure is well replicated. This behaviour is calibrated by adopting an extensional stiffness of the connectors K_c equal to 1,500 N/mm. The tension field development inside the plate before the failure is shown in Figure 6, and it is possible to observe that the FEM model is able to simulate the stress concentration in the panel corners.

The final results of the calibration phase are listed in Table 2 in terms of initial stiffness (K_i), maximum shear force (F_{max}) and total energy dissipated during the testing process ($E_{d,tot}$). As the experimental test results on the more slender panels have shown a dependence from both the initial

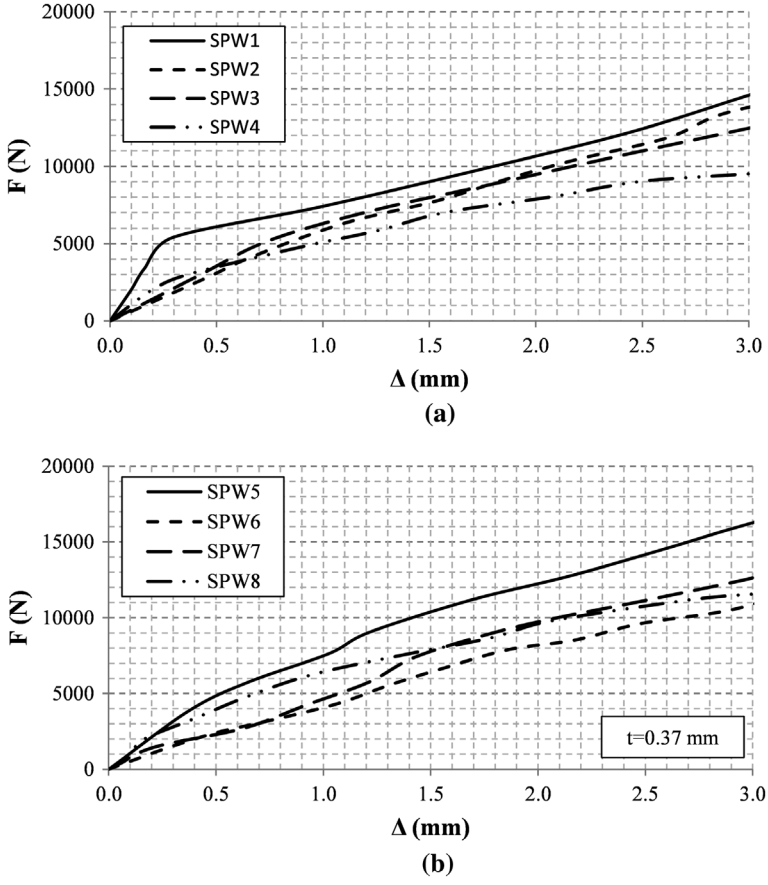

Figure 7. Experimental initial curves of the panels tested by Valizadeh et al. (2012) having thickness equal to 0.70 mm (a) and (b) 0.37 mm (b). Despite a larger hole diameter, SPW8 panel showed an apparently initial curve stiffer than the other perforated panels: this may be due to the initial slipping under the first load increment.

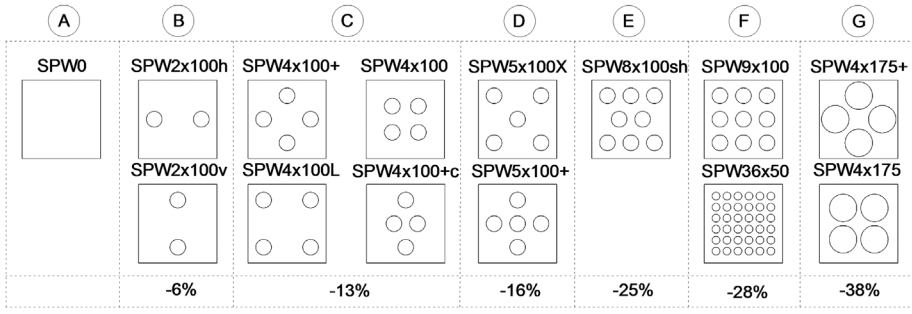

Figure 8. Groups of analysed panels and identification of drilling percentages. The acronym SPW is followed by: the number of holes, the hole diameter (mm) and a symbol identifying the hole pattern (v: vertical, h: horizontal, L: large, +: vertical cross, c: close, X: diagonal cross, s: staggered).

Table 3. Mechanical properties of materials used in the parametric analysis. A conventional yielding strength at 0.2% strain level is adopted

Material	E (MPa)	ν	f_y (MPa)	f_u (MPa)	ε_u
Steel	200,000	0.3	180	300	0.15
Aluminium (AW 1050A)	70,000	0.3	18	70	0.35

buckling for low load levels and the initial slipping (i.e. SPW6 and SPW7 panels), a secant stiffness at the displacement of 3 mm is conventionally assumed for a more realistic representation of the initial experimental behaviour of the panels (see Figure 7). Under with these assumptions, the results have shown that the FEM model is able to satisfactorily simulate the behaviour of shear panels in terms of stiffness. The comparison between experimental and numerical results in terms of strength for SPW6 and SPW7 panels has shown a greater difference due to the lack of modelling of the fracture observed around the holes during the experimental tests (see Figure 5). Less accuracy is also observed in simulating the pinching effect, due to local instabilities occurrence. However, the FEM model can be considered as sufficiently reliable, as it accurately estimates the three basic parameters (K_i, F_{max}, $E_{d,tot}$) characterizing the physical behaviour of the panels coming from the experimental evidences.

3.3. Parametric analysis

A number of 13 different configurations of perforated shear panels and one without holes are analysed in the present study. The full shear panel is considered as a reference specimen to be compared with the perforated panels. The drilled configurations differ from each other in terms of location, number and diameters of holes (Figure 8), material (steel or aluminium) and plate thickness. In particular, following the dimensions of the specimens tested by Valizadeh et al. (2012), steel plates with a thickness of 0.37, 0.70 and 1.40 mm are considered. In addition, aluminium plates with thickness of 3.70 and 7.00 mm are analysed in order to promote also the use of aluminium for MPSW systems. The choice of the aluminium plates thickness is made in order to cover the same resistance range of steel panels.

The mechanical characteristics of the used materials are shown in Table 3. Since the FEM model calibration has been done on the basis of existing tests, the same steel quality is adopted for parametric analyses. The mechanical properties of aluminium correspond to an “ad hoc” material obtained by a thermal treatment, as suggested by De Matteis, Formisano, Mazzolani, and Panico (2008), which lowers the elastic limit and amplifies the ultimate elongation. The plate-to-frame connections are analogous to that used by Valizadeh et al. (2012), with a calibrated mean value of the connectors axial stiffness equal to 1,200 N/mm. Any possible crisis of the plate-to-frame connections is not taken into account in the model since the failure should not occur in such areas for perforated configurations. The plates initial imperfection are given with an out-of-plane deformation having amplitude of 1 mm according to the panel first instability mode already considered in the previous FEM analysis phase. In the same way of the experimental tests, the FEM analyses are

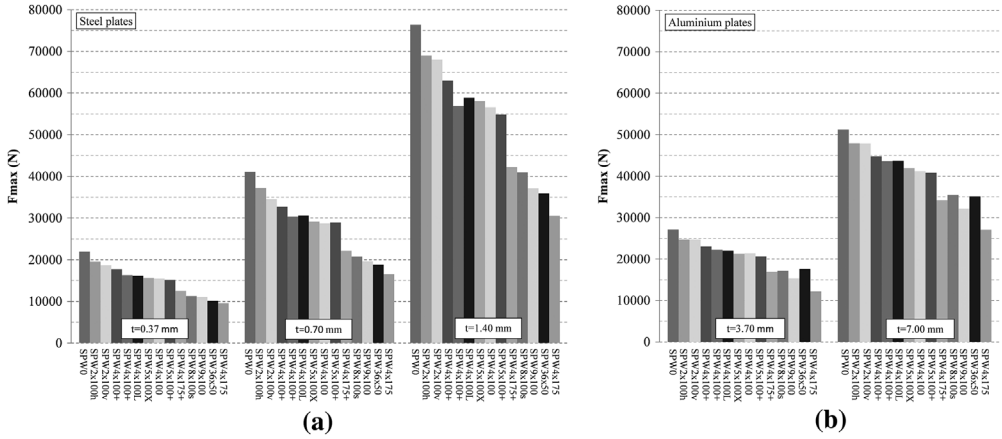

Figure 9. Comparison between analysed steel panels (a) and aluminium panels (b) in terms of shear strength.

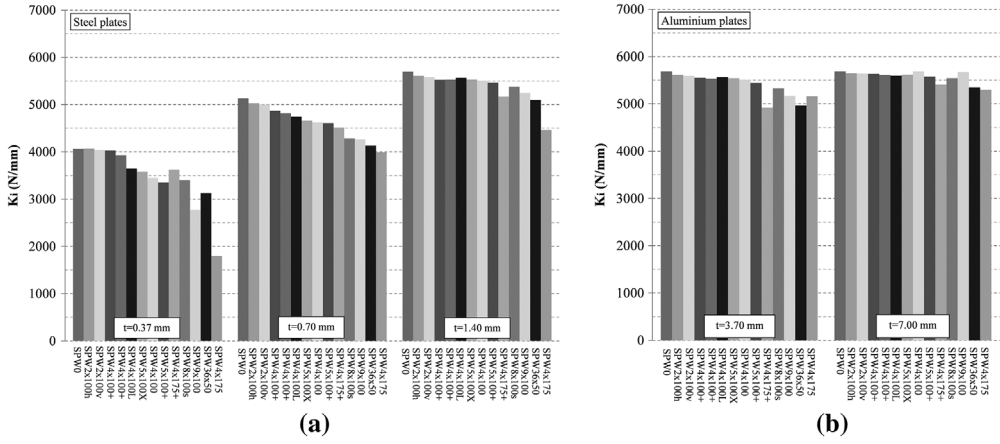

Figure 10. Comparison between analysed steel panels (a) and aluminium panels (b) in terms of initial stiffness.

pushed until either the creation of fractures around holes or the accomplishment of the maximum allowable displacement (drift of 6%) are attained.

Figures 9 and 10 provide a summary of the contribution offered by steel and aluminium plates in terms of maximum reached shear force and initial stiffness, respectively. A large variety of strength contribution of steel and aluminium perforated panels, lower than those offered by full panels, can be identified in these figures. This can be an advantage because the choice of an appropriate drilling configuration of the plates can lead to the desired level of strength improvement in the structure where panels are inserted. By taking the aluminium plates with the same drilling configuration, but with a thickness 10 times greater than the steel plate one, a uniform initial stiffness is shown due to a less weakening effect.

For the sake of example, the comparisons in terms of hysteretic curves for three panels having a percentage of holes ($\rho_{holes} = A_{holes}/A_{sup}$) equal to 6, 16 and 28% are, respectively, reported in Figures 11–13. From these figures, it is noticed that aluminium panels have a better dissipative behaviour than the steel ones. For the former panels, the hysteretic cycles appear to be larger and characterized by both negligible pinching effect and absence of fractures around the holes. This is due to the different mechanical properties of the materials, which cause the adoption of aluminium plates thicker than steel ones. For steel plates, a thickness equal to 1.40 mm is necessary to reach the 6% drift without the formation of cracks around the holes, with the exception of drilling configurations with holes very close each to other (i.e. SPW4 × 100 + c, SPW4 × 175+, SPW8 × 100 sh).

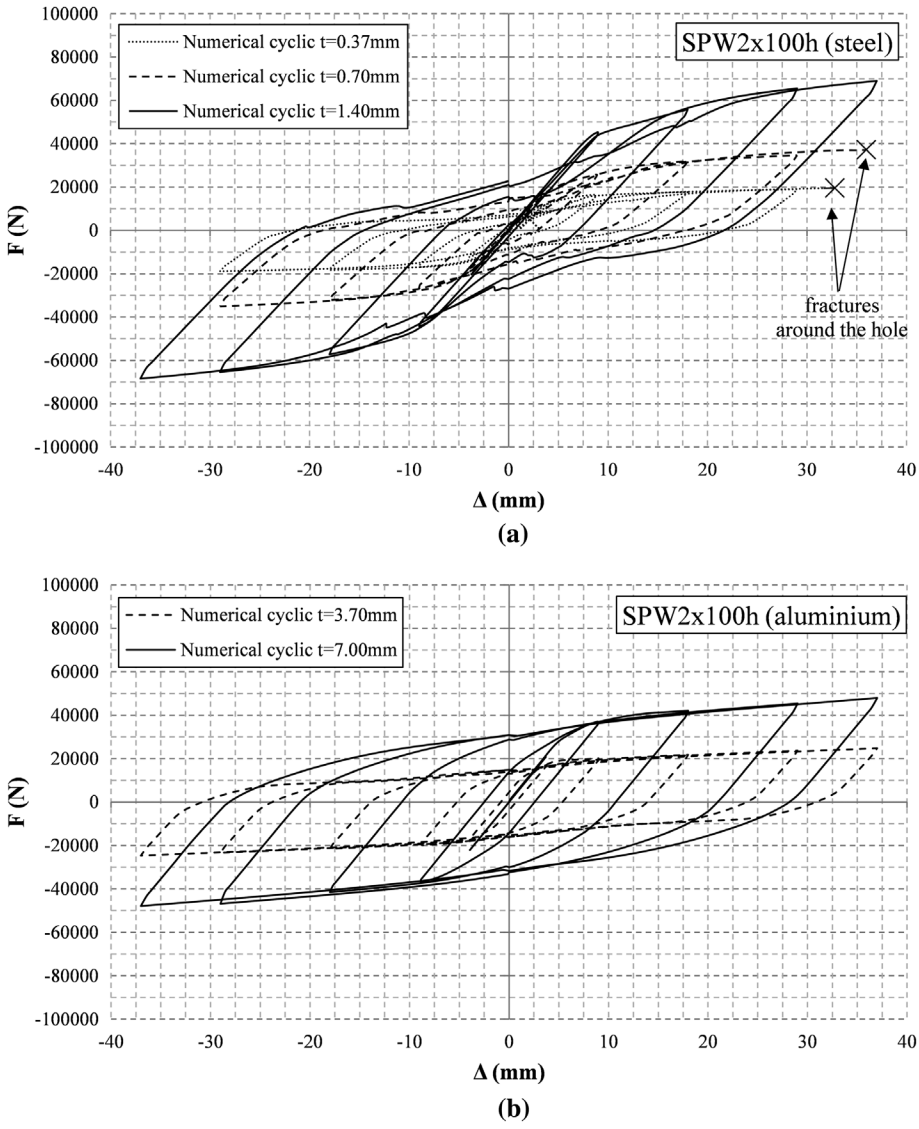

Figure 11. Hysteretic curves of SW2 × 100h steel (a) and aluminium (b) panels with different thicknesses.

As shown in Figure 14, despite the presence of holes that hinder the formation of the tension field, the inclination of the tensile bands in all panels is substantially of 45°. Compared to full panels, the number of active bands decreases and it is reduced to one in the case of centred holes (i.e. SPW4 × 100 + c, SPW4 × 100, SPW4 × 175, SPW4 × 175+). Furthermore, there is always a different activation of the yielding mechanism with respect to full panels. In fact, yielding activates around the holes in perforated panels, without stressing the system joints, while yielding is activated in corner zones in full SPSWs, penalizing the connection systems. It is also possible to notice that, a considerable reduction of the stress state in the perimeter area is found in the perforated panels with a high percentage of holes.

3.4. The proposed design charts

On the basis of the obtained numerical results, the design charts reported in Figure 15 are proposed to evaluate the modification factors C_{m1} and C_{m2}, which appear in Equations 3 and 4 proposed by Sabouri-Ghomi et al. (2005), to correctly predict the non-linear behaviour of perforated panels. These factors are obtained by assuming a simplified bi-linear force–displacement curve, which comes from the envelope of the numerical cyclic behaviour by compensating the areas (Figure 16). To do this, a

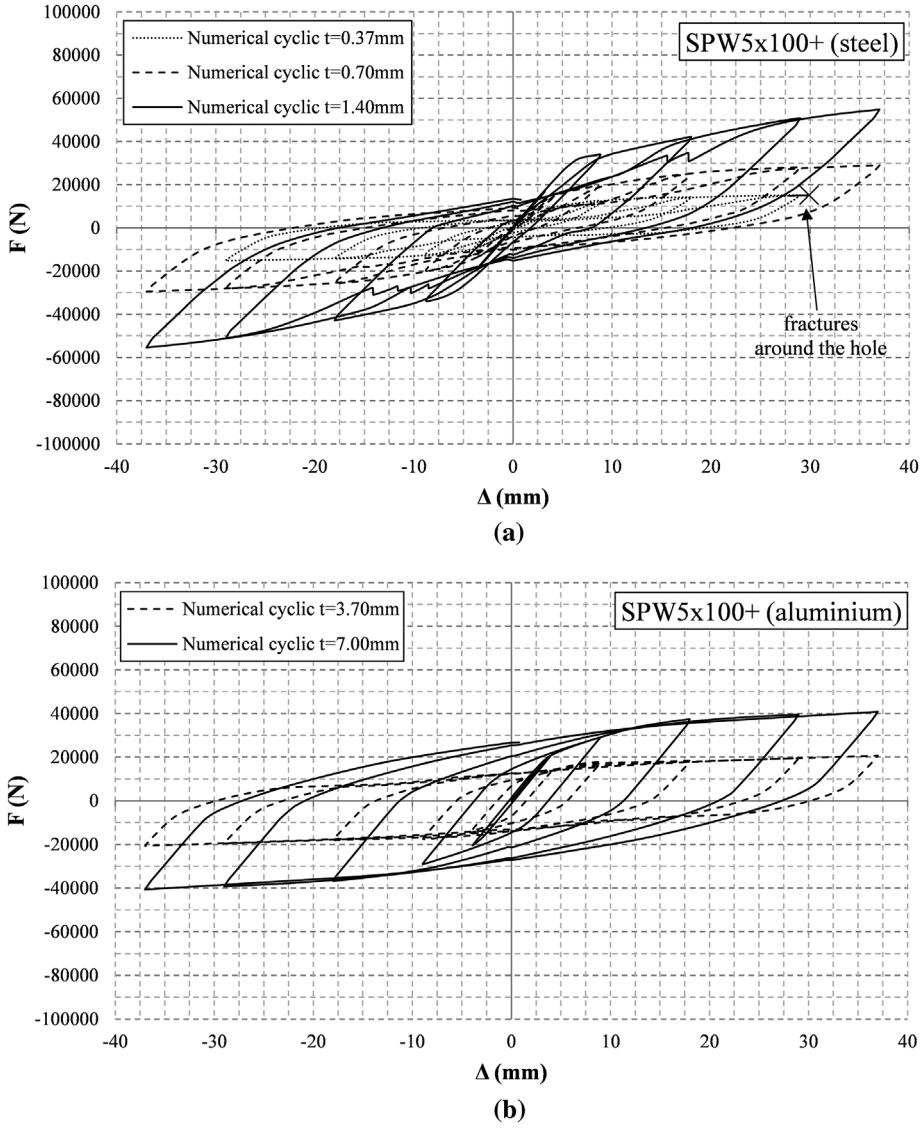

Figure 12. Hysteretic curves of SW5 × 100+ steel (a) and aluminium (b) panels with different thicknesses.

secant stiffness K_w^* at 3 mm of displacement is fixed on numerical curves in order to obtain the correspondent unknown shear strength F_{wu}^* by the following equation:

$$A = \frac{F_{wu}^* \Delta_y^*}{2} + F_{wu}^* (\Delta_{max} - \Delta_y^*) \tag{7}$$

where A is the area under each curve up to the maximum displacement Δ_{max}, which correspond to either the formation of fractures around the holes or the achievement of the maximum drift (6%), while Δ_y^* is the conventional yielding displacement of the bi-linear curve, which can be expressed as F_{wu}^*/K_w^*. Then, the unknown shear strength is obtained as follows:

$$F_{wu}^* = K_w^* \left[\Delta_{max} \pm \sqrt{\Delta_{max}^2 - \frac{4A}{2K_w^*}} \right] \tag{8}$$

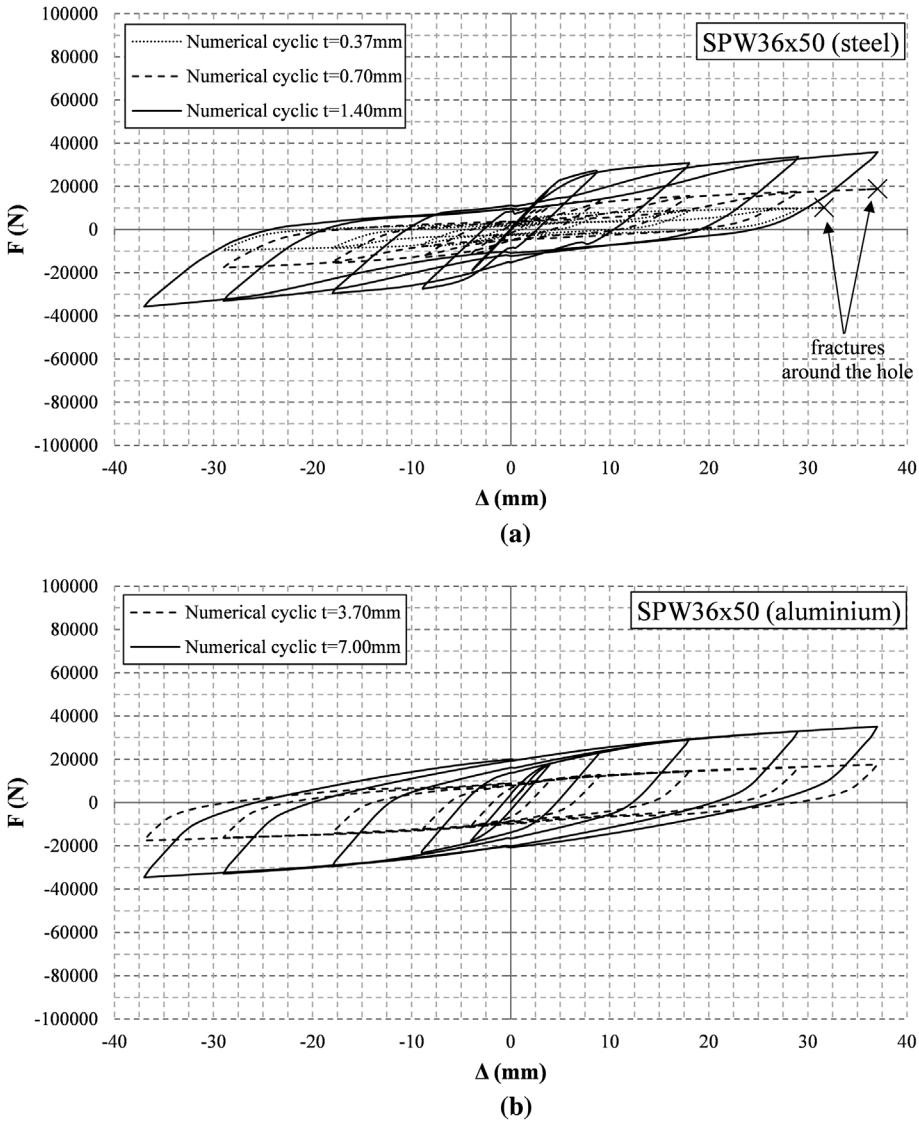

Figure 13. Hysteretic curves of SW36 × 50 steel (a) and aluminium (b) panels with different thicknesses.

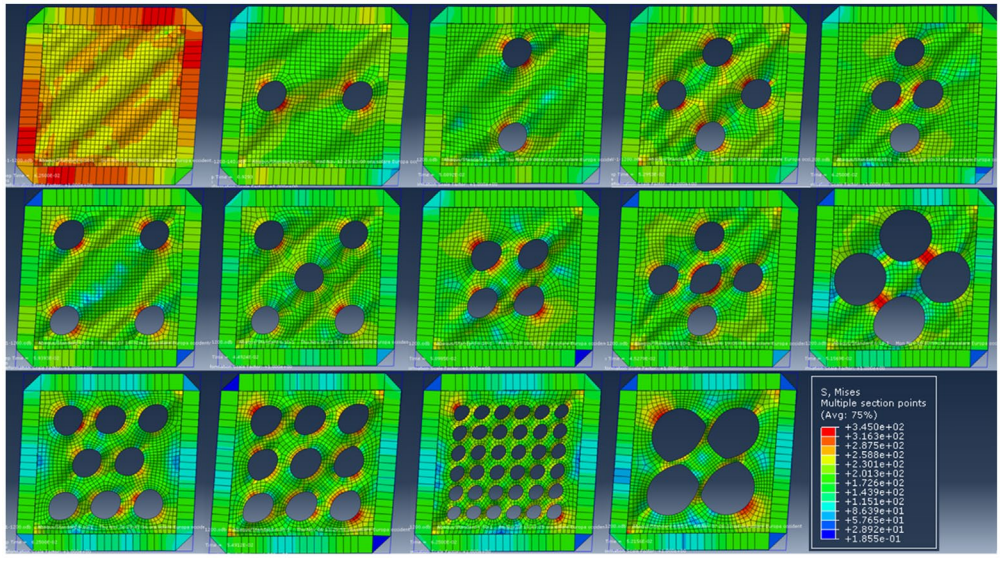

Figure 14. Final stress and deformation states of the analysed steel shear panels.

Note: The values of the legend refer to the steel true stress of the panel systems.

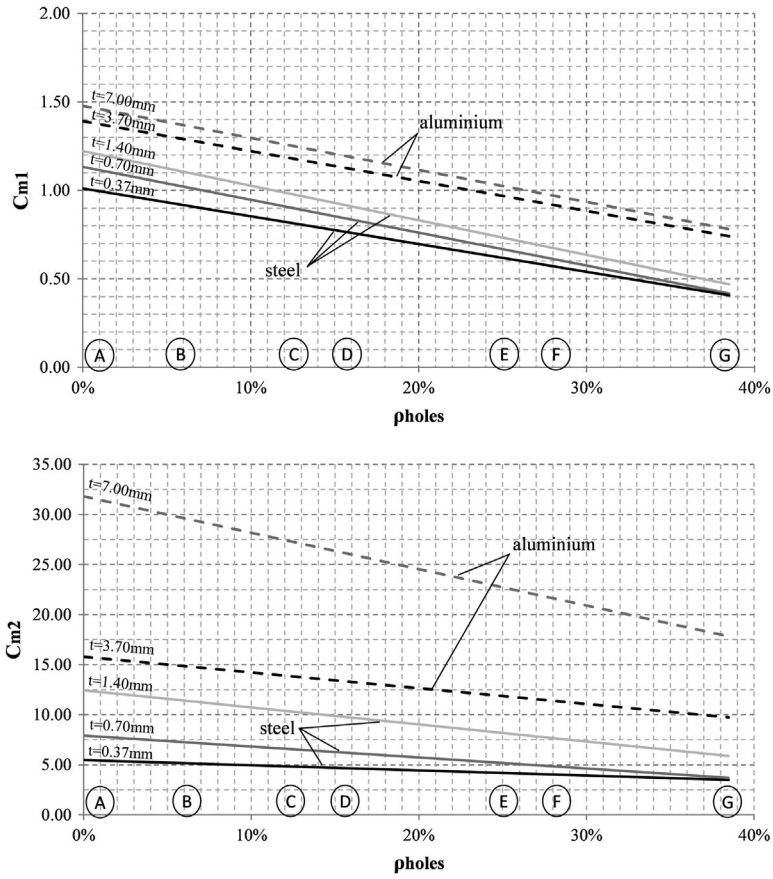

Figure 15. Design charts for estimating the correction factors used to predict the non-linear behaviour of SPSWs.

Note: The letters from A to G correspond to the perforated panel types identified in Figure 8 on the basis of the percentage of holes.

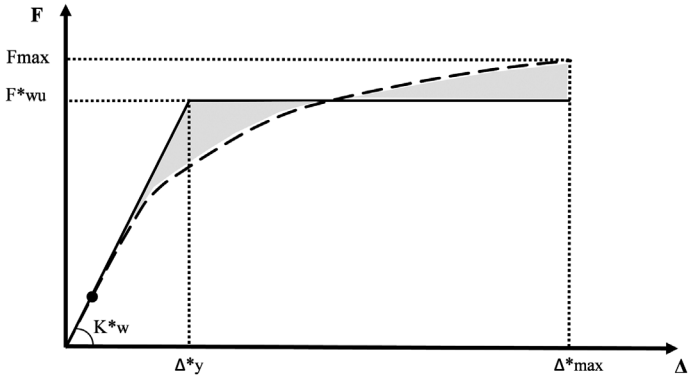

Figure 16. Bi-linearization of the numerical cyclic curve envelope.

Once the characteristic values of the bi-linear curves are calculated, the modification factor C_{m1} and C_{m2} are obtained (by matching first Equations 1–3 and after Equations 2–4) and a linear trend can be plotted in the design charts of Figure 15.

In the same figure, it is shown that the values of C_{m1} and C_{m2} for aluminium are always higher than the ones used for steel. These trends can be due to the different mechanical properties of such materials (aluminium has an hardening ratio f_u/f_y that is about 2.33 times the steel one and a Young modulus E that is about 1/3 of the steel one), but also to the aluminium plates thicknesses assumed in the analyses, which are greater than those used for steel plates. In fact, the aluminium panel stiffness reduction appears to be smaller than the steel panel one by increasing the percentage of holes.

4. Concluding remarks

The results of a wide FEM study on unstiffened perforated metal plate shear panels within pinned boundary frames are presented in this paper. The available experimental results on panels with a central opening have allowed to set up and calibrate an appropriate FEM model, where geometric imperfections and material non-linearity have been considered. The presence of the bolted plate-to-frame connections and their imperfections have been also taken into account with a simple method, based on axial connectors with a behaviour properly calibrated on the basis of experimental tests. This calibration phase of the FEM model has guaranteed to obtain a satisfactory numerical-to-experimental agreement in terms of both the overall behaviour and the consequential deformed shape of the system.

On this consolidated basis, a parametric FEM analysis on panels with different perforation patterns, material and thickness has been carried out. The different perforation patterns have been considered by modifying location, number and diameter of the holes. Moreover, steel plates with thicknesses of 0.37, 0.70 and 1.40 mm and aluminium plates with thicknesses of 3.70 and 7.00 mm have been adopted for numerical analyses. From the results, it is observed that, despite the presence of holes, the inclination of tension field essentially remains about 45°, but the number of active bands, depending on the location of holes, decreases in comparison to the full panel one. Furthermore, the activation mode of the yielding mechanism is favourable for perforated panels, as it occurs in the areas around the holes instead of the perimeter zones, like for full panels, so to avoid to penalize the connection systems. In particular, a considerable reduction of the stresses in the perimeter area is found in perforated panels with a high percentage of holes. In addition, by adopting thicker perforated plates, very large drifts can be attained without fractures around holes that lead to decrease both the shear strength and the energy dissipation capacity of these devices. When aluminium plates are used for MPSW systems, plates thicker than steel ones are needed due to both the low conventional yielding strength and the Young modulus of the aluminium alloys. In this case, panels show a more dissipative behaviour than steel panel ones, with large drifts reached without failures and hysteretic curves afflicted by a negligible pinching effect. However, the production costs of aluminium plates may limit their employment in practical applications.

Finally, a useful analytical tool has been proposed for professional users. Based on design formulas for the estimation of the shear strength and initial stiffness of traditional shear panels with pinned joint frames, design charts have been suggested for the evaluation of modification factors taking into account the presence of various drilling configurations. Although such design charts are valid for panels having only the same plate geometry and materials of the ones herein examined, the exposed procedure can be generalized to any case. In fact, since perforated MPSWs with proper perforation patterns can be a viable alternative to traditional system for strengthening and stiffening of both new and existing structures, similar design charts could be proposed into National Codes for the accurate design of these lateral load-resisting systems.

Funding
The authors received no direct funding for this research.

Author details
A. Formisano[1]
E-mail: antoform@unina.it
ORCID ID: http://orcid.org/0000-0003-3592-4011
L. Lombardi[1]
E-mail: luca.lombardi@bristol.ac.uk
[1] Department of Structures for Engineering and Architecture, University of Naples "Federico II", P.le Tecchio 80, 80125 Naples, Italy.

Citation information
Cite this article as: Numerical prediction of the non-linear behaviour of perforated metal shear panels, A. Formisano & L. Lombardi, *Cogent Engineering* (2016), 3: 1156279.

References

Astaneh-Asl, A. (2000, February). Steel plate shear walls. *Proceedings, U.S.-Japan Partnership for Advanced Steel Structures, U.S.-Japan Workshop on Seismic Fracture Issues in Steel Structures*. San Francisco, CA.

Basler, K. (1961). Strength of plate girders in shear. *Journal of the Structural Division (ASCE), 87*, 150–180.

Berman, J. W., & Bruneau, M. (2005). Experimental investigation of light-gauge steel plate shear walls. *Journal of Structural Engineering, 131*, 259–267. http://dx.doi.org/10.1061/(ASCE)0733-9445(2005)131:2(259)

Bhowmick, A. K., Grondin, G. Y., & Driver, R. G. (2014). Nonlinear seismic analysis of perforated steel plate shear walls. *Journal of Constructional Steel Research, 94*, 103–113. http://dx.doi.org/10.1016/j.jcsr.2013.11.006

Brando, G., & De Matteis, G. (2014). Design of low strength-high hardening metal multi-stiffened shear plates. *Engineering*

Structures, 60, 2–10. http://dx.doi.org/10.1016/j.engstruct.2013.12.005
Dassault Systèmes. (2010). ABAQUS 6.10. Providence, RI: Simulia Corp.
De Matteis, G., Formisano, A., & Mazzolani, F. M. (2009). An innovative methodology for seismic retrofitting of existing RC buildings by metal shear panels. *Earthquake Engineering and Structural Dynamics, 38*, 61–78. http://dx.doi.org/10.1002/eqe.v38:1
De Matteis, G., Formisano, A., Mazzolani, F. M., & Panico, S. (2005, January). Design of low-yield metal shear panels for energy dissipation. *Proceedings of the Final Conference of COST ACTION C12*. Innsbruck, Austria, 665–675.
De Matteis, G., Formisano, A., Mazzolani, F. M., & Panico, S. (2008). Numerical and experimental analysis of pure aluminium shear panels with welded stiffeners. *Computers & Structures, 30*, 545–555.
Formisano, A., De Matteis, G., & Mazzolani, F. M. (2010). Numerical and experimental behaviour of a full-scale RC structure upgraded with steel and aluminium shear panels. *Computers and Structures, 88*, 1348–1360. http://dx.doi.org/10.1016/j.compstruc.2008.09.010
Formisano, A., De Matteis, G., Panico, S., Calderoni, B., & Mazzolani, F. M. (2006, August). Full-scale test on existing RC frame reinforced with slender shear steel plates. *Proceedings of the 5th International Conference on Behaviour of Steel Structures in Seismic Areas – STESSA 2006* (pp. 827–834). Yokohama.
Formisano, A., De Matteis, G., Panico, S., & Mazzolani, F. M. (2008). Seismic upgrading of existing RC buildings by slender steel shear panels: A full-scale experimental investigation. *Advanced Steel Construction, 4*, 26–45.
Formisano, A., & Lombardi, L. (2015, September). Perforated shear panels for seismic rehabilitation of existing reinforced concrete buildings. *Proceedings of the Fifteenth International Conference on Civil, Structural and Environmental Engineering Computing*. Prague, Czech Republic: Civil-Comp Press.
Formisano, A., Mazzolani, F. M., Brando, G., & De Matteis, G. (2006, August). Numerical evaluation of the hysteretic performance of pure aluminium shear panels. *The 5th International Conference on Behaviour of Steel Structures in Seismic Areas (STESSA '06)*. Yokohama, Japan.
Formisano, A., Mazzolani, F. M., & De Matteis, G. (2007). Numerical analysis of slender steel shear panels for assessing design formulas. *International Journal of Structural Stability & Dynamics, 7*, 273–294.
Formisano, A., & Sahoo, D. R. (2015). Steel shear panels as retrofitting system of existing multi-story RC buildings: Case studies. *Advances in Structural Engineering: Mechanics, 1*, 495–512. doi:10.1007/978-81-322-2190-6_41, ISBN: 978-813222190-6;978-813222189-0
Hitaka, T., & Matsui, C. (2003). Experimental study on steel shear wall with slits. *Journal of Structural Engineering, 129*, 586–595. http://dx.doi.org/10.1061/(ASCE)0733-9445(2003)129:5(586)
Mistakidis, E. S., De Matteis, G., & Formisano, A. (2007). Low yield metal shear panels as an alternative for the seismic upgrading of concrete structures. *Advances in Engineering Software, 38*, 626–636. http://dx.doi.org/10.1016/j.advengsoft.2006.08.043
Purba, R., & Bruneau, M. (2007). *Design recommendations for perforated steel plate shear walls* (Technical Report No. MCEER-07-0011). Buffalo: Multidisciplinary Center for Earthquake Engineering Research, State University of New York.
Roberts, T. M., & Sabouri-Ghomi, S. (1991). Hysteretic characteristics of unstiffened plate shear panels. *Thin-Walled Structures, 12*, 145–162. http://dx.doi.org/10.1016/0263-8231(91)90061-M
Roberts, T. M., & Sabouri-Ghomi, S. (1992). Hysteretic characteristics of unstiffened perforated steel plate shear panels. *Thin-Walled Structures, 14*, 139–151. http://dx.doi.org/10.1016/0263-8231(92)90047-Z
Sabouri-Ghomi, S., Ventura, C. E., & Kharrazi, M. H. K. (2005). Shear analysis and design of ductile steel plate walls. *Journal of Structural Engineering, 131*, 878–889. http://dx.doi.org/10.1061/(ASCE)0733-9445(2005)131:6(878)
Thorburn, L. J., Kulak, G. L., & Montgomery, C. J. (1983). *Analysis of steel plate shear walls* (Structural Engineering Report No. 107). Edmonton: Department of Civil Engineering, University of Alberta.
Timoshenko, S. P., & Gere, J. M. (1961). *Theory of elastic stability*. New York, NY: McGraw-Hill Book Company.
Valizadeh, H., Sheidaii, M., & Showkati, H. (2012). Experimental investigation on cyclic behavior of perforated steel plate shear walls. *Journal of Constructional Steel Research, 70*, 308–316. http://dx.doi.org/10.1016/j.jcsr.2011.09.016
Xue, M., & Lu, L. W. (1994, June). Interaction of infilled steel shear wall panels with surrounding frame members. *Proceedings of 1994 Annual Task Group Technical Session, Structural Stability Research Council: Reports on Current Research Activities*. Bethlehem, PA: Lehigh University.